ESD-TR-87-267

Project Report
CMT-105

Evaluation of a Wideband Direction Estimation Algorithm for Acoustic Arrays

T. Peli

11 February 1988

Lincoln Laboratory
MASSACHUSETTS INSTITUTE OF TECHNOLOGY
LEXINGTON, MASSACHUSETTS

**Prepared for the Department of the Air Force
under Electronic Systems Division Contract F19628-85-C-0002.**

The work reported in this document was performed at Lincoln Laboratory, a center for research operated by Massachusetts Institute of Technology, with the support of the Department of the Air Force under Contract F19628-85-C-0002.

This technical report has been reviewed and is approved for publication.

FOR THE COMMANDER

Hugh L. Southall

Hugh L. Southall, Lt. Col., USAF
Chief, ESD Lincoln Laboratory Project Office

MASSACHUSETTS INSTITUTE OF TECHNOLOGY
LINCOLN LABORATORY

EVALUATION OF A WIDEBAND DIRECTION ESTIMATION ALGORITHM FOR ACOUSTIC ARRAYS

T. PELI
Group 21

PROJECT REPORT CMT-105

11 FEBRUARY 1988

LEXINGTON MASSACHUSETTS

Abstract

Simulated data has been used to evaluate the performance of an acoustic target detection and direction estimation algorithm. The signals used to test the algorithm were simulated acoustic signals propagating across a nine-sensor, tri-delta array. Band-limited broadband sources as well as periodic sources were simulated. The outputs of the algorithm consisted of azimuth and power estimates along with a quantity intended as a quality measure for the azimuth estimates.

The accuracy of azimuth estimates was examined for single sources. Cumulative Probability Density Functions (CPDF) of azimuth estimate deviation were computed as a function of input signal-to-noise ratio (SNR) and the parameters of the algorithm. For an harmonic source the error was always less than 5 deg, and for a wideband source less than 1.5 deg. The relationship between the standard deviation of azimuth estimates and the output quality measure was determined for various parameter settings and the two types of sources. The quality measure was not sensitive to source type, but it was affected by the processing parameters. The quality measure can be useful in estimating the error when tuned to a set of processing parameters.

The minimum azimuth separation required to resolve two wideband sources was measured as a function of the input SNR and compared to the nominal resolution of the array. At 40 dB SNR, the minimum azimuth separation was 6 deg; it increased to 15 deg at 0 dB SNR. The resolution achieved by the wideband algorithm was always better than the predicted nominal resolution. For multiple sources, the maximum number of widely spread wideband sources which can be resolved was measured as a function of input SNR. At 40 dB SNR, 6 targets can be resolved; the number decreases to 4 at 0 dB SNR.

Detection and false alarm probabilities were computed as a function of a detection threshold applied to the quality factor produced by the algorithm. This was done for a range of input SNRs and up to six targets. The results suggest that 3 is a good threshold to use. High P_D, low P_{FA}, good target resolution, and a large number of detectable targets are achieved using this threshold.

The performance of the wideband algorithm was compared to the well-known Maximum Likelihood Method (MLM) using single targets. For a wideband source the estimates of the wideband algorithm were as good as or better than the estimates of the MLM algorithm. For an harmonic source MLM performs better when source harmonics are known.

TABLE OF CONTENTS

LIST OF ILLUSTRATIONS

LIST OF TABLES

1. INTRODUCTION

An acoustic target detection and direction estimation algorithm for small microphone arrays has been developed by Nawab et al. [1]. This algorithm can be used to detect and determine source directions for multiple airborne sound sources, and it may have application in systems that employ small microphone arrays to detect and locate low-flying air vehicles. The algorithm utilizes all of the source signal energy, even when the energy is spread over a wide bandwidth. Hence,the algorithm is called wideband. It is a high-resolution algorithm with modest computational requirements. The computational load is on the order of that for the Maximum Likelihood Method (MLM) algorithm [2] for a single frequency. These features and initial results reported by Nawab et al. [1] motivated a detailed investigation of the performance of the algorithm. The results of that investigation are presented in this report.

The accuracy of azimuth estimates for a single source and the ability to handle multiple sources have been examined. Single source accuracy was measured as a function of input signal-to-noise ratio (SNR), angle quantization in calculating direction, source types, and the values of the parameters of the algorithm. All measurements were for a specific, 9-element, 6-m aperture microphone array. The azimuth separation required to resolve two sources, and the maximum number of widely spread (in azimuth space) sources that can be resolved, were measured as a function of input SNR.

Algorithm outputs include a quality measure to indicate the reliability of directional estimates. The usefulness of the quality measure was tested through simulations. The performance of the new algorithm was also compared to that of the MLM algorithm.

2. ALGORITHM DESCRIPTION

This section contains a summary description of the wideband (WB) algorithm, with emphasis on its important parameters. Additional theory and details are presented in [1].

The theoretical basis of the method depends upon the properties of spatial covariance functions and their Fourier transforms. At any time t_o, a plane wave propagating from bearing Θ and elevation $\emptyset$ has a constant value along any horizontal line orthogonal to the direction Θ. The spatial autocovariance function in the horizontal plane has the same property. The Fourier transform of that spatial covariance function, which is the zero-delay wave number spectrum, has its energy concentrated along a ridge passing through the origin with an angle Θ. The ridge has two arms; one in the Θ direction, and one in the $\Theta + 180$ direction. One arm corresponds to negative, and the other to positive frequencies. For real signals there is an ambiguity between Θ and $\Theta + 180$. This ambiguity can be avoided by using the complex analytic representation for the signals, which removes negative frequency components. With the 180° ambiguity removed, the process of detection and direction finding reduces to finding radial ridges. The strength of a source is the integral of the values along the radial ridge.

There are three phases to the wideband algorithm: (a) prefiltering and estimation of a zero-delay covariance matrix, (b) spatial spectrum analysis to obtain the zero-delay wave number spectrum, and (c) detection of ridges and directions.

The estimation of the zero-delay covariance matrix is done using a few seconds of data. This involves dividing the data into small blocks,

computing a sample of the Complex Analytic Representation (CAR) [3] for the signals in each block, forming a zero delay covariance matrix estimate for each block, and averaging over blocks.

Figure 1 illustrates breaking the data into blocks and calculating the CARs, a_i^k, for the k^{th} block and the i^{th} data channel. The zero delay covariance matrix estimate for the k^{th} block is given by the outer product.

$$R^k = \begin{vmatrix} a_1^k(a_1^k)^* & a_1^k(a_2^k)^* & \cdots & a_1^k(a_m^k) \\ \vdots & \vdots & & \vdots \\ a_n^k(a_1^k)^* & \cdots & & a_n^k(a_n^k)^* \end{vmatrix} \qquad (1)$$

The signals may also be filtered as part of the CAR process, and the blocks in a time segment can be overlapped to improve SNR.

Any number of techniques can be used to perform the spectrum analysis in the second step of the wideband (WB) algorithm. The method used in this report is the Maximum Likelihood Method developed originally by Capon for narrow band applications. It can be applied without modification to the wideband problem. Thus, the zero-delay wave number spectrum $P(k_x, k_y)$ is given by

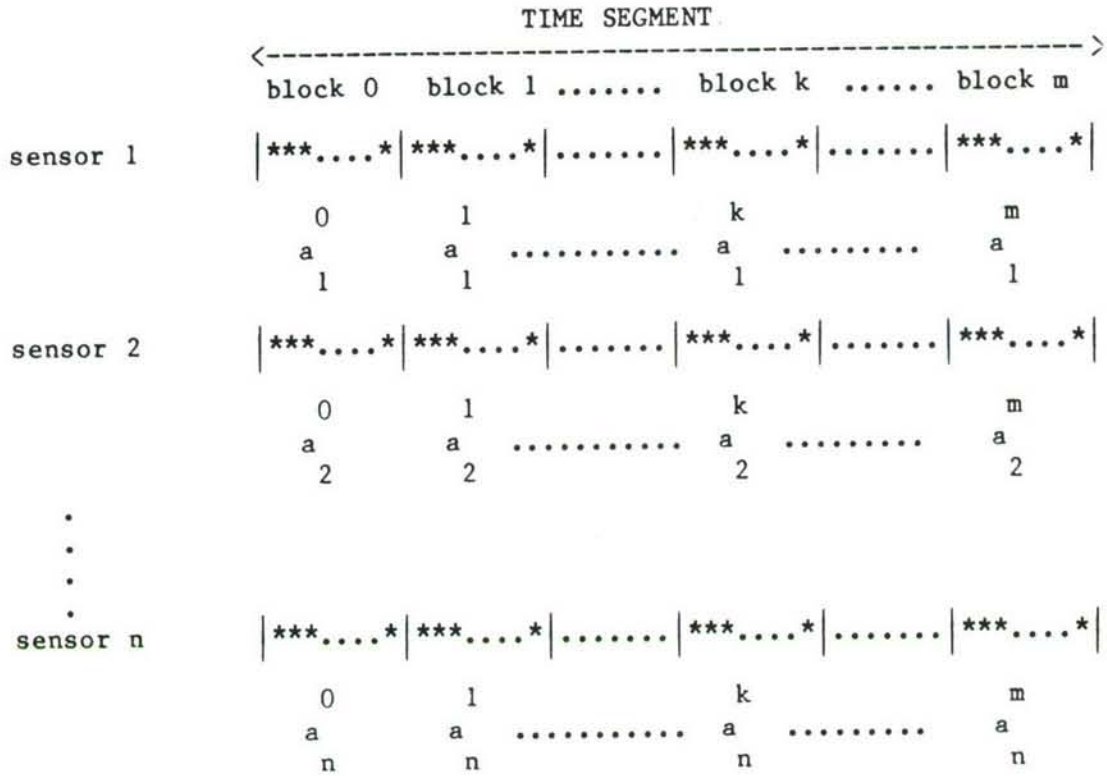

Figure 1. Data segmentation for covariance matrix estimation.

$$P(k_x,k_y) = \frac{1}{E^H R^{-1} E} \qquad (2)$$

where E is a steering vector, which is a function of sensor location and wave number (k_x,k_y), H denotes Hermitian transpose and R is the estimated zero delay covariance matrix.

The final step is to average power along each direction (azimuth) in the two-dimensional wave number space to generate a 1-D power estimate of the form shown in Figure 2 and to determine source directions by choosing the highest peaks. The data shown in Figure 2 are from a live experiment with two aircraft. The situation at the time corresponding to the data is shown in the insert. The two aircrafts were barely resolvable at that time. Peaks corresponding to the aircraft are labeled. Smaller peaks are a combination of noise and sidelobes.

The basic direction estimates do not provide any measure of their quality, although quality estimates are required by acoustic tracking algorithms. An ad hoc quality measure was defined and tested to determine its possible utility for tracking algorithms. The quality measure of a direction estimate is defined as the ratio of the power from that direction divided by an overall noise power estimate. The noise power is estimated as the average of the lowest 5% of the values in the averaged power signal. Since it is a ratio of two positive numbers, it is bounded from below by zero. In general, small values correspond to low SNR conditions, and high values to high SNR conditions.

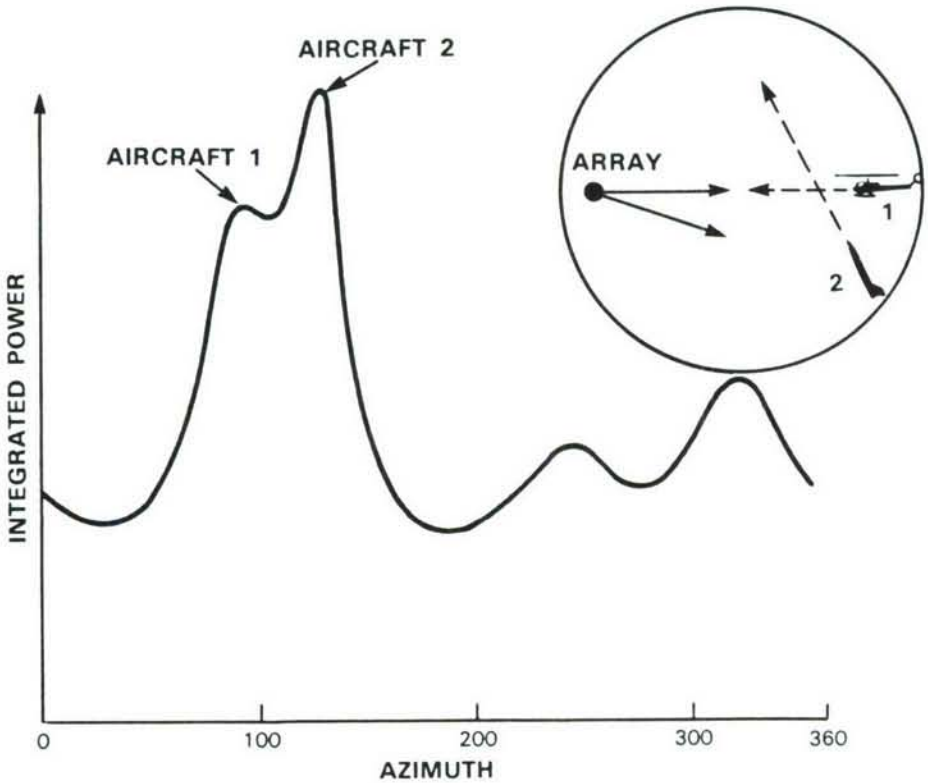

92994-2

Figure 2. General view of radially averaged power.

3. SIMULATED DATA

Monte Carlo experiments with synthetic acoustic data were used to obtain the results in this report. Each experiment consisted of many computer runs, ranging from 20 to 100 in number, using different data for each run. The processing parameters and statistics of the data were the same for all runs during a single experiment. For each experiment the results from all the runs were averaged to estimate the performance corresponding to the processing parameters and signal statistics for the experiment.

All experiments were performed using two seconds of synthetic data sampled at 2048 samples per second. For each run in each experiment a single signal was synthesized for each source, and delayed copies were made to represent the propagation across the tri-delta array shown in Figure 3. In all of the simulations the signal was assumed to arrive horizontally. For single source simulations the source was toward the East (90° azimuth).

Two types of sources were examined; wideband and harmonic. The wideband source was band limited white noise. It roughly approximates the signal from a jet aircraft. The harmonic source was a weighted sum of harmonic sine waves. The harmonic source roughly approximates the signals from a helicopter.

Various amounts of white noise were added to the signals to produce different SNRs. The input SNR in dB is defined as 20 times the logarithm of the ratio of the root-mean-square (RMS) value of the signal to the RMS value of the noise.

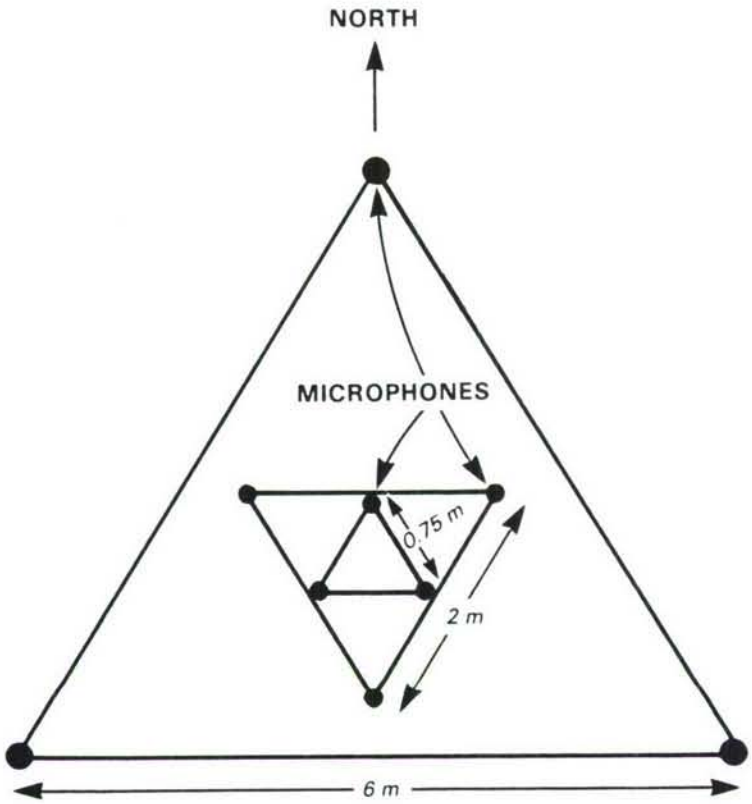

92994-3

Figure 3. Nine-sensor tri-delta array.

All results in this report are given in terms of input signal to noise ratio as just defined. However the effective SNR may differ from this because of prefilters that were used for different experiments. The SNR gains (or losses) due to prefiltering are summarized in Table I. These can be added to input SNRs to obtain the net in-band SNRs available at the array input.

TABLE I

SNR GAIN ATTRIBUTED TO PREFILTERING

Signal Model		Prefiltering Band	SNR Gain
Wideband	a	100-200	4
	b	50-100	12
Harmonic	a	16-200	7
		96-200	-4
	b	10-100	10

a - sources for section 4

b - sources for section 5

4. PERFORMANCE OF THE WIDEBAND ALGORITHM

This section presents WB algorithm performance results for four situations:

a. single harmonic source
b. single wideband source
c. two wideband sources
d. multiple wideband sources

All of the results presented here and in Section 5 are in terms of input SNR. The input SNR is the most natural measure to use. It is fixed by the type of the aircraft, the aircraft range, background noise and the wind conditions, etc. The results could have been given in terms of output SNR. This has not been done largely due to the complexity of the algorithm. There is at this time no practical way to calculate output SNR from a description of the input signals and the processing.

Although there is no simple way to calculate the effective output SNR for the different test situations it is possible to make a few comments about the sources of SNR gain, in addition to those contained in the Section 3 concerning prefiltering.

One source of SNR gain is array processing gain such as one obtains from any phased array system. This gain is highly variable, depending upon signal and noise statistics and the exact form of the array and the algorithm. An often used nominal value for array gain is 10 log N where N is the number of sensors; microphones in our case. This is about 9 dB for a nine element array like the tri-delta array used for our Monte Carlo experiments with simulated data. Thus when reasonably good performance is quoted for an input SNR of only 0 dB it should be no surprise since the

array will nominally provide 9 dB of SNR gain. The results cited below are all for N = 9.

Other sources of SNR gain, but ones that are even more difficult to quantify are the gain resulting from temporal averaging to estimate zero-delay covariance matrices and the gain resulting from radial integration in wave number space. Each is a different form of incoherent integration that reduces random fluctuations in the output. The following results explicitly address some effects of temporal averaging but not the effects of wave number averaging.

4.1 Single Harmonic Source

Direction finding accuracy was measured for a single harmonic signal consisting of sine waves of decaying amplitudes (Figure 4), propagating from an azimuth of 90 deg. We examined the accuracy of the azimuth estimates as a function of the input SNR and various values of the block size and the prefiltering frequency band. Azimuth was quantized into 0.25 deg steps. For each SNR 100 computer runs were made, each using 2 s of simulated data. In each run the peak with the best quality was assigned as the estimate. Except for a few cases at 0 dB SNR, the peak with the best quality was always the nearest peak to the true direction.

The effect of the block size and overlap was investigated with signals prefiltered to pass only positive frequencies in the 16 to 200 Hz band. Power was estimated as a function of azimuth using nonoverlapping blocks of 128, 256 points, and 256 points with 50% overlap. The data in all cases consisted of two seconds of signals sampled at 2048 samples per second.

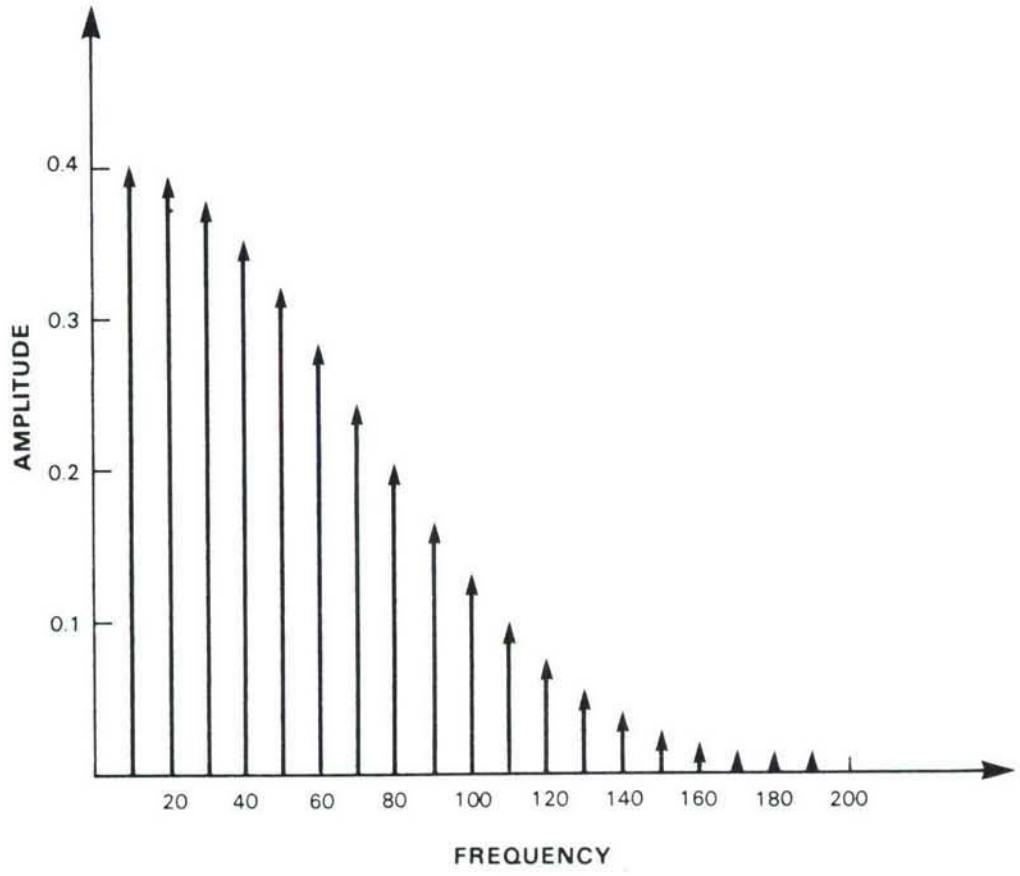

Figure 4. Amplitudes of sine waves of a harmonic signal as a function of temporal frequency.

Thus, the number of blocks was 32 for a block size of 128 and was 16 or 24 for a block size of 256, depending on the overlap. The results are shown in Figure 5(a-c) as a function of input SNR. Values in parentheses are average values of the output quality measure. The prefiltering SNR gain is 7 dB as indicated in Table I.

For each block size the accuracy decreases as the input SNR decreases. Best results were obtained with a 128 block size. In that case, even at a low SNR, i.e., 0 dB, errors were always within 5 deg. The worst performance was obtained using a 256 block size with no overlap. The main reason for the difference in performance is that a block size of 128 provides more statistical averaging; twice as much if nonoverlapping blocks are statistically independent. That results in a better estimate of the sensor cross-covariances matrix. The results of Figure 5(c) are intermediate between the two other cases. In that case some additional statistical stability was obtained with overlapped blocks. In general, for a fixed interval time of estimation, short blocks provide more block averaging, which reduces noise. Larger blocks provide for more accurate calculation of the complex analytic representation of the signal and rejection of unwanted frequency components.

The effect of a different prefiltering band has also been investigated. The signals were prefiltered to 96-200 Hz, which is a high frequency subband of the 16-200 Hz frequency band, using a 128 block size. In these cases the SNR after prefiltering was actually reduced by 4 dB (see Table I).

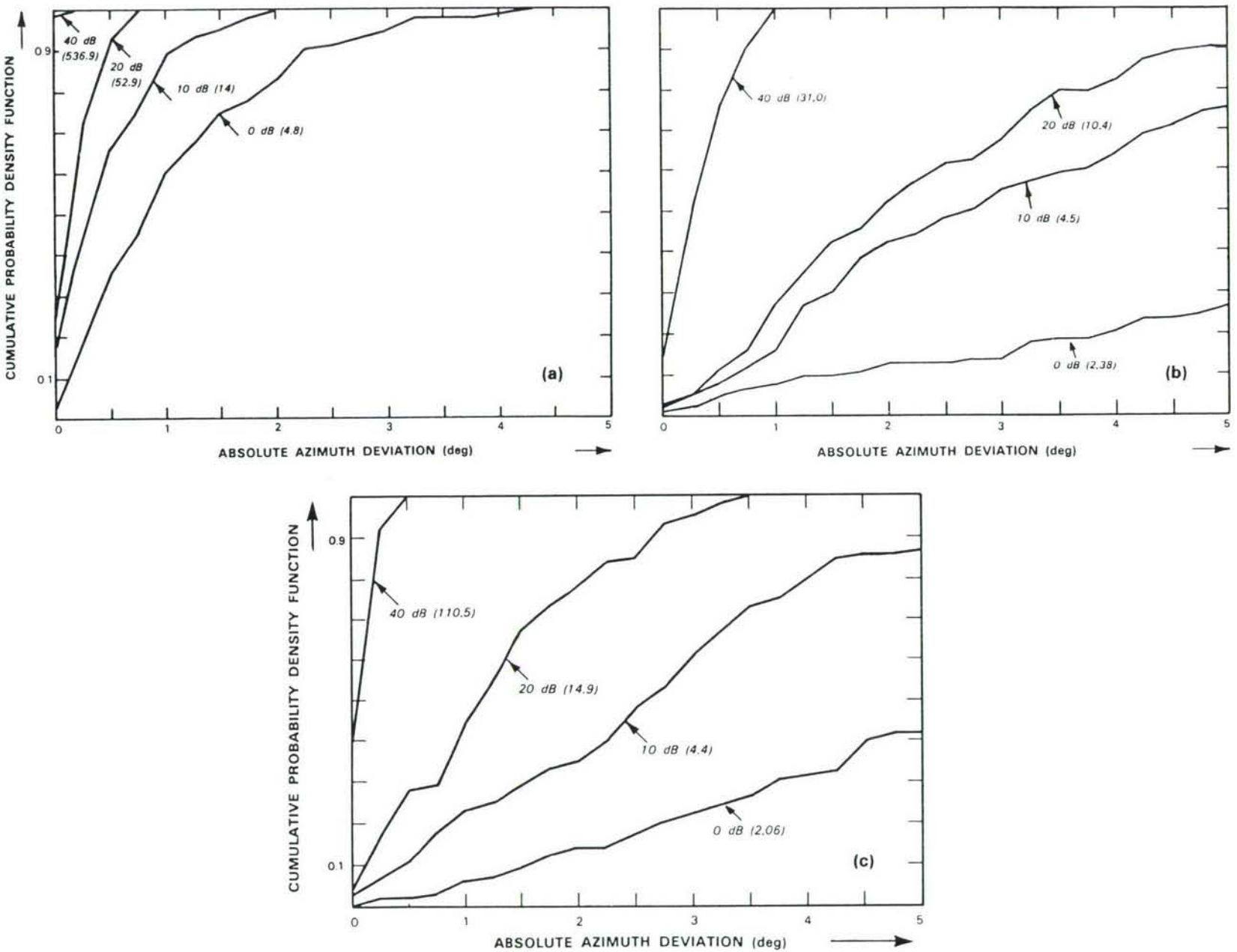

Figure 5. Cumulative probability density function (CPDF) of azimuth estimates deviation at 40, 20, 10, and 0 dB input SNR and for a harmonic signal prefiltered to 16-200 Hz. (a) 128 block size, (b) 256 block size, (c) 256 block size with 50% overlap; in parentheses are average values of the output quality measure.

The cumulative probability density function of the errors as a function of input SNR is given in Fig. 6. The estimates are even more accurate at high SNR than the estimates shown in Fig. 5(a). At 0 dB SNR the azimuth estimates are about the same as Fig. 5(a). The improvement in the estimates results from ability of the algorithm to concentrate on only the higher frequencies, for which a fixed size array has a better inherent accuracy [4-5]. In Fig. 5(a) the algorithm had to concentrate on both low and high frequencies. Prefiltering to a higher band actually reduced the effective input SNR as a consequence of the exponential decay of signal power as a function of frequency. But for this experimental case the increased array resolution more than compensated for the loss of SNR.

Figure 7 illustrates, for a harmonic signal, the relation between the quality measure and the standard deviation of azimuth estimates. The statistics for Fig. 7(a) are a compilation from all previous simulations, i.e., results with different parameters are included. Figure 7(b) illustrates the results for the specific case of a 128 block size and 96 - 200 Hz frequency band. The values of the standard deviation are much lower than in Fig. 7(a), and the decrease in standard deviation with increasing quality measure is more consistent. The performance and relationship of the quality measure and the standard deviation of the estimates are affected by the processing parameters, but the quality measure can be calibrated to provide a useful estimate of standard deviation for any specific set of processing parameters.

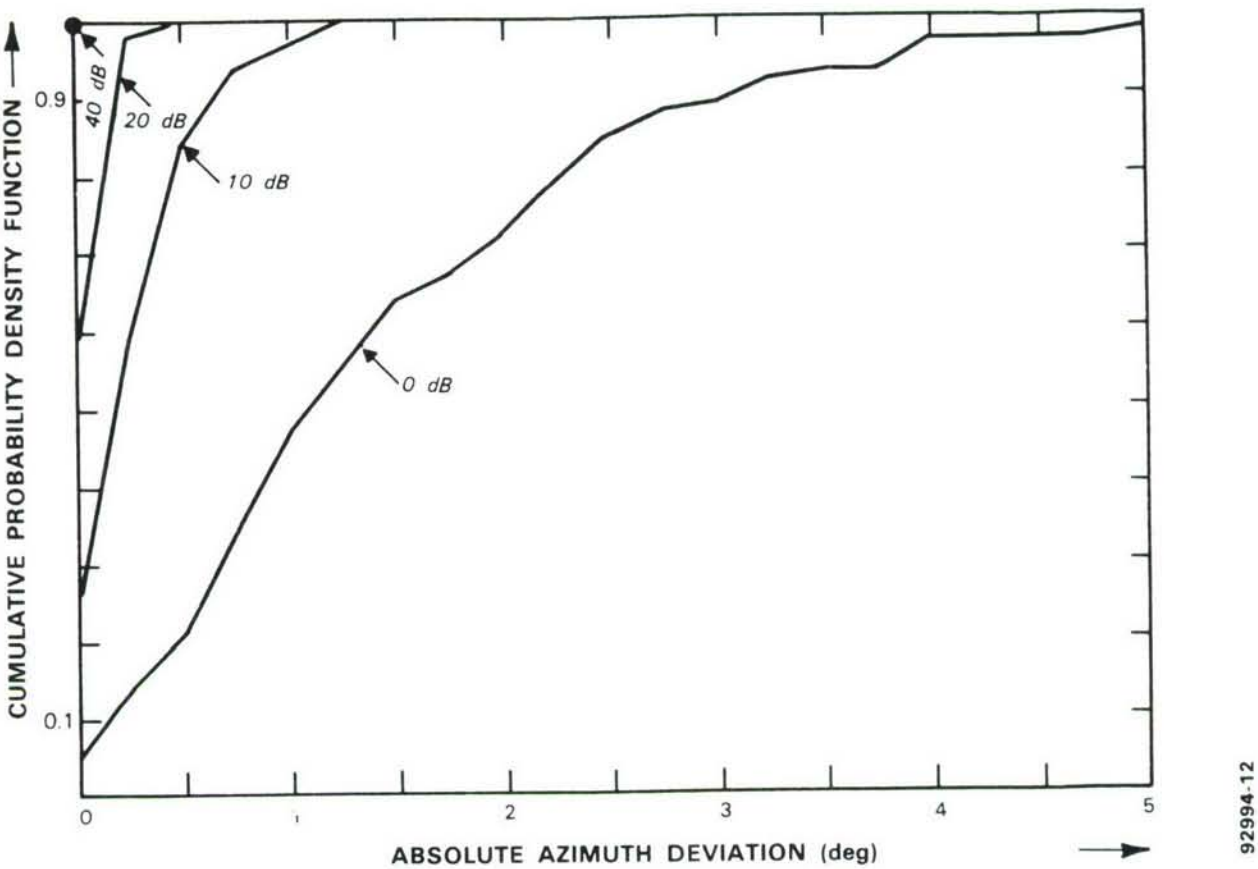

Figure 6. Cumulative probability density function of azimuth estimates deviation as a function of input SNR for a harmonic signal prefiltered to 96 - 200 Hz.

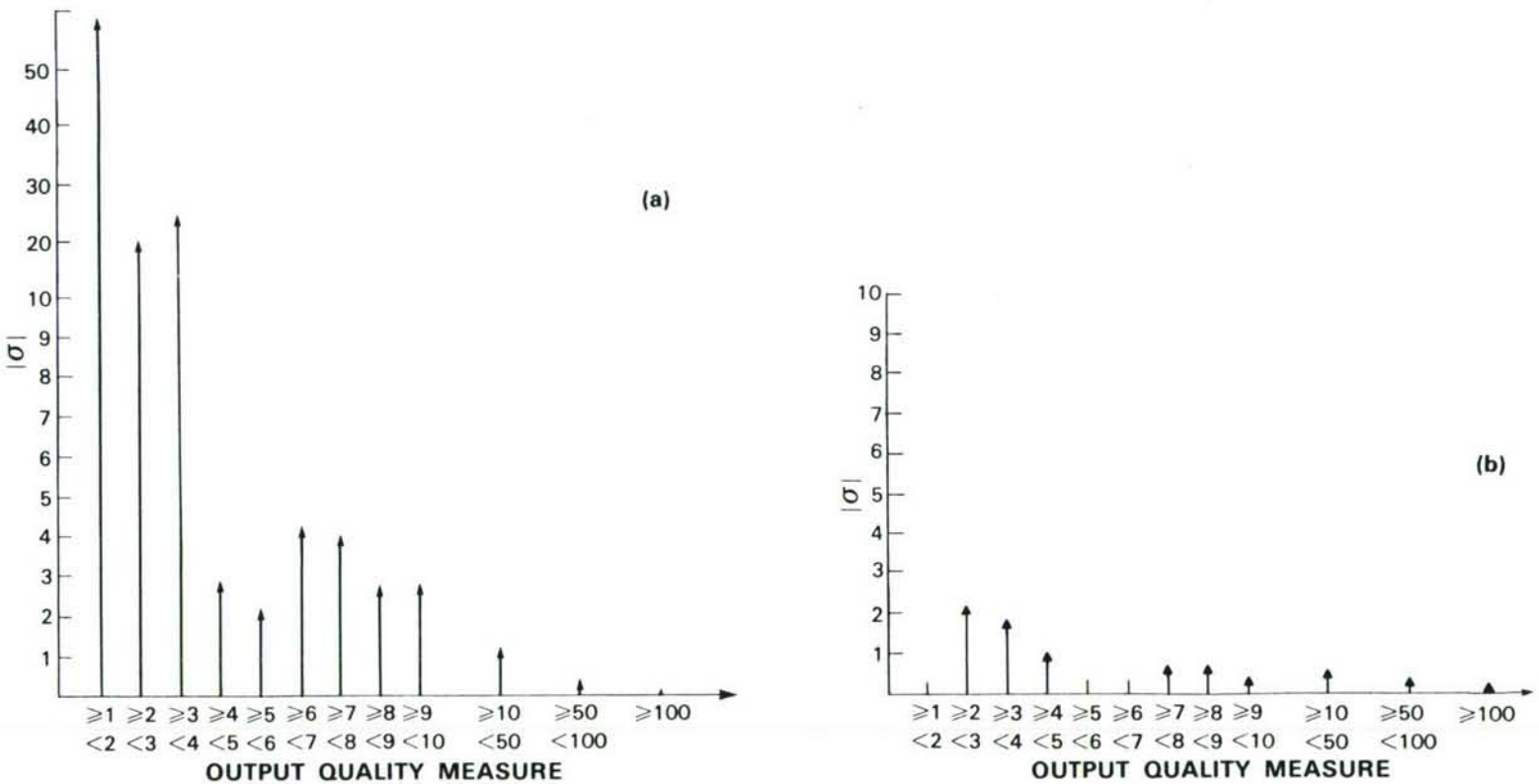

Figure 7. Standard deviation of azimuth estimates as a function of the output quality measure for a harmonic source. (a) Using all the results, (b) using a 128 block size and 96 - 200 Hz prefiltering frequency band.

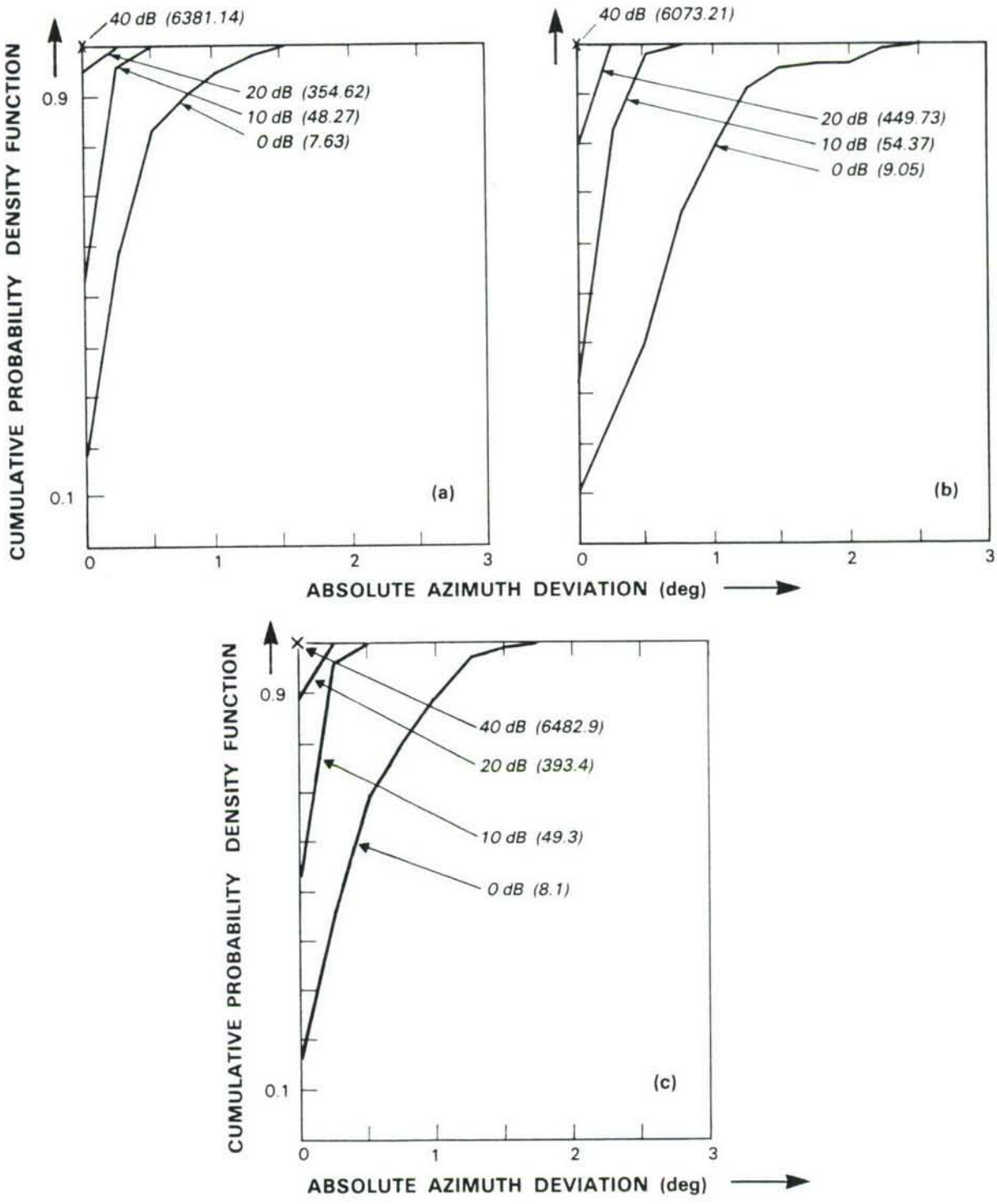

Figure 8. Cumulative probability density function of azimuth estimates deviation as a function of SNR for a wideband source prefiltered to 100-200 Hz. (a) 128 block size, (b) 256 block size, (c) 256 block size with 50% overlap.

4.2 Single Wideband Source

The wideband test signal was white noise in the band 50-500 Hz. The signal plus noise was prefiltered to the 100-200 Hz frequency band, and performance measured as a function of input SNR and block size. The 100-200 Hz frequency band was used because it is believed to be a good all purpose band for aircraft detection. Prefiltering to this band for these tests gave a SNR gain of 4 dB (see Table I). Accuracy was measured as a function of input SNR and block size. The output peak with the best quality was chosen as the estimate. It also was the nearest peak to the true direction in every case.

The results are shown in Figure 8(a-c). Best performance was again obtained with a 128 block size, although a block size of 256 points with 50% overlap gave very similar results. The worst performance was obtained using a 256 block size with no overlap. At 0 dB SNR the azimuth errors were less than 1.5 deg for a 128 block size, less than 2 deg for a 256 block size with 50% overlap and less than 2.5 deg for a 256 block size with no overlap. Once again, accuracy decreases as the SNR decreases.

Comparing Fig. 8 with Fig. 5, it is evident that the performance is much better for the wideband source than for the harmonic source. It is also reflected by the higher values of the quality measure for a wideband source than for a harmonic source.

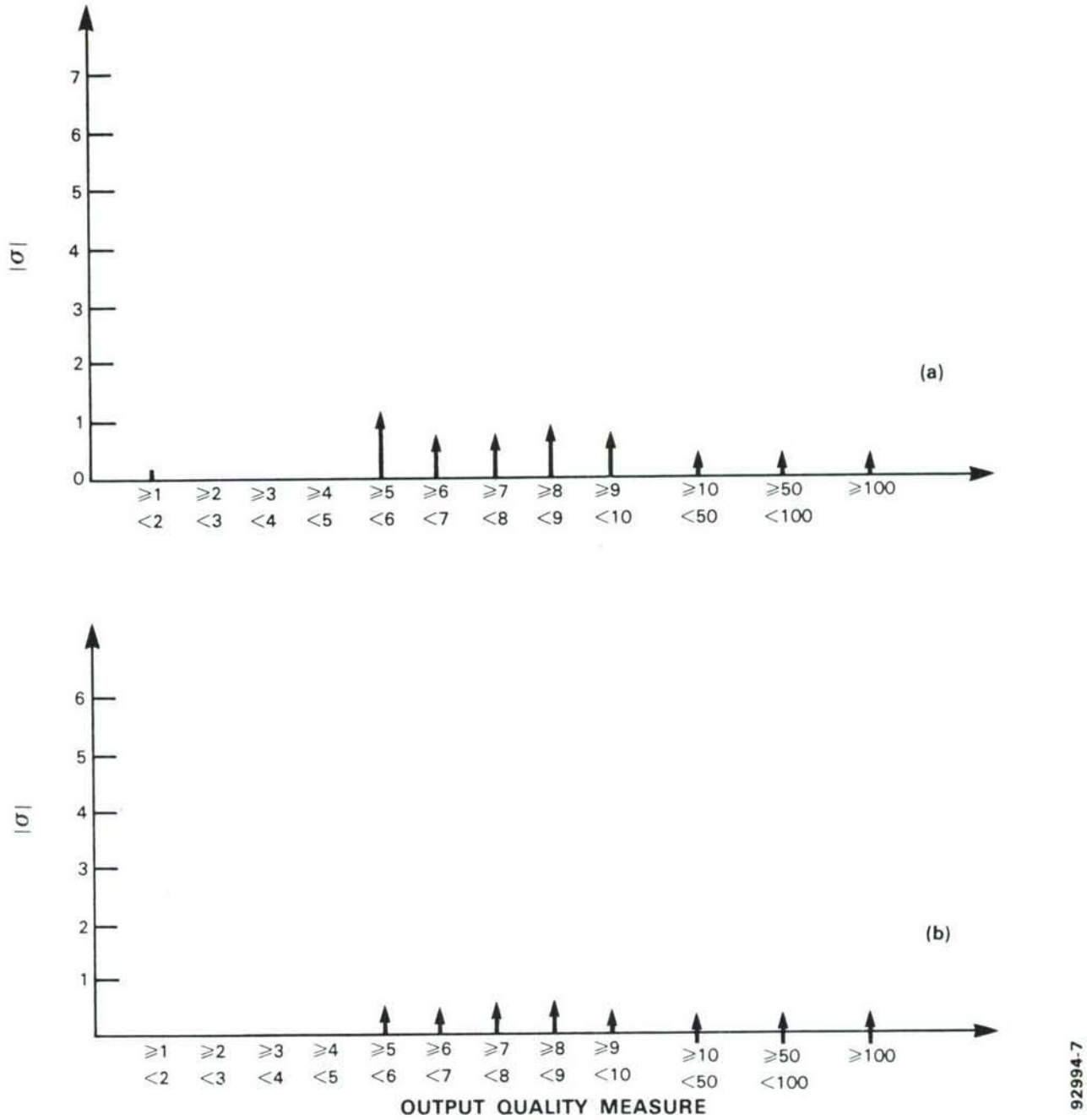

Figure 9. Standard deviation of azimuth estimates as a function of the output quality measure for a wideband source. (a) Using all results, (b) using results of a 128 block size.

Figure 9(a) illustrates the relation between the output quality measure and the standard deviation σ for a wideband source, independent of block size and overlap. The relationship between σ and the output quality for a 128 block size is given in Fig. 9(b). Comparing the results of Fig. 7(b) and Fig. 9(b), Fig. 7(b) contains more low values of the quality measure for the same range of input SNR. But σ as a function of the quality measure is comparable, which means that the quality measure is not overly sensitive to source type.

4.3 Single Source Detection and False Alarm Probabilities

The accuracy results in Sections 4.1 and 4.2 were obtained by associating the highest quality peak in the signal processor output with the known signal source. No detection threshold was applied to the output quality measure. Table II shows that the effect of a detection threshold applied to the dimensionless positive signal quality measure is minimal for a single wideband target in noise. With $t = 0$, which corresponds to no threshold, there were always secondary peaks and therefore false alarms. For all other threshold values that were tested the experimental false alarm rate fell to zero. Only for the lowest SNR and highest detection threshold values did the detection statistics fall below unity. The results indicated that for the SNR values tested, a threshold of 3-4 will significantly reduce false alarms without reducing detection probabilities.

4.4 Minimum Azimuth Separation Between Two Wideband Sources

The smallest resolvable azimuth separation (quantized to 3 deg) between two equal power wideband sources has been determined as a function of input SNR. The results were obtained from 50 runs (simulations) for

TABLE II(a)

PROBABILITY OF DETECTION FOR A SINGLE WIDEBAND SOURCE

	t = 0	t = 3	t = 4	t = 6	t = 8
SNR = 40 dB	1.0	1.0	1.0	1.0	1.0
SNR = 30 dB	1.0	1.0	1.0	1.0	1.0
SNR = 20 dB	1.0	1.0	1.0	1.0	1.0
SNR = 10 dB	1.0	1.0	1.0	1.0	1.0
SNR = 0 dB	1.0	1.0	1.0	0.91	0.32

TABLE II(b)

PROBABILITY OF FALSE ALARM FOR A SINGLE WIDEBAND SOURCE

	t = 0	t = 3	t = 4	t = 6	t = 8
SNR = 40 dB	1.0	0.0	0.0	0.0	0.0
SNR = 30 dB	1.0	0.0	0.0	0.0	0.0
SNR = 20 dB	1.0	0.0	0.0	0.0	0.0
SNR = 10 dB	1.0	0.0	0.0	0.0	0.0
SNR = 0 dB	1.0	0.0	0.0	0.0	0.0

each azimuth separation. In these simulations, two targets were declared resolved if their azimuth estimates had the highest quality measures values of all the peaks. The minimum azimuth separation was defined as the smallest separation for which two targets were resolved with probability of at least 0.9 (i.e., 45 out of 50 runs). All simulations were conducted with the same block size and frequency band as for the single wideband source (a 128 block size and signals prefiltered to the 100 - 200 Hz band).

Figure 10 shows the experimentally obtained minimum azimuth separation as a function of input SNR. It is 6 deg at 40 dB SNR and increases to 15 deg as the SNR is reduced to 0 dB. These results compare very favorably with results predicted by the nominal beamwidth of the array.

The nominal angular beamwidth of an array is

$$\theta = 2 \arctan ((\pi/D)/k) \qquad (3)$$

where

$k = 2\pi f/c$,

f = frequency,

c = velocity of sound 340 m/s,

and

D = the aperture of the array.

Figure 11 shows θ as a function of frequency for different apertures. In our simulations D was equal to 6 m. The nominal beamwidth is also the nominal resolution of an array. If two equal power signals are separated by a full beamwidth or more they will usually result in two distinct peaks in the array output as a function of angle. Thus, the two sources will be

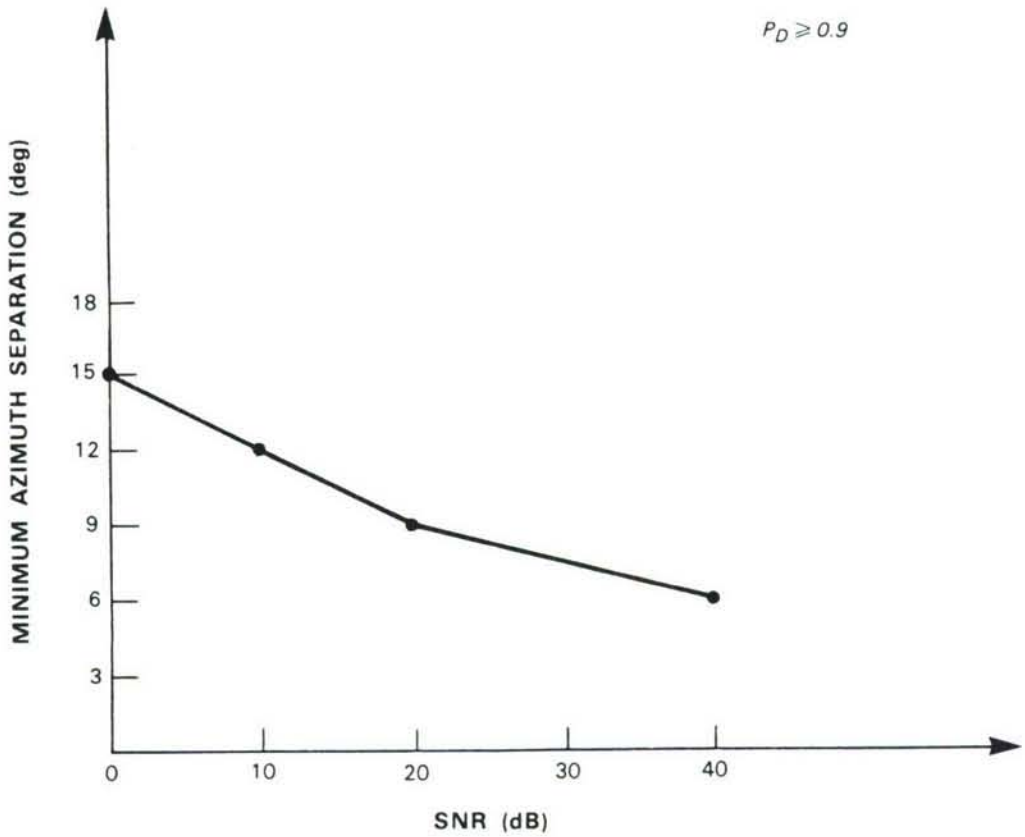

Figure 10. Minimum azimuth separation as a function of input SNR.

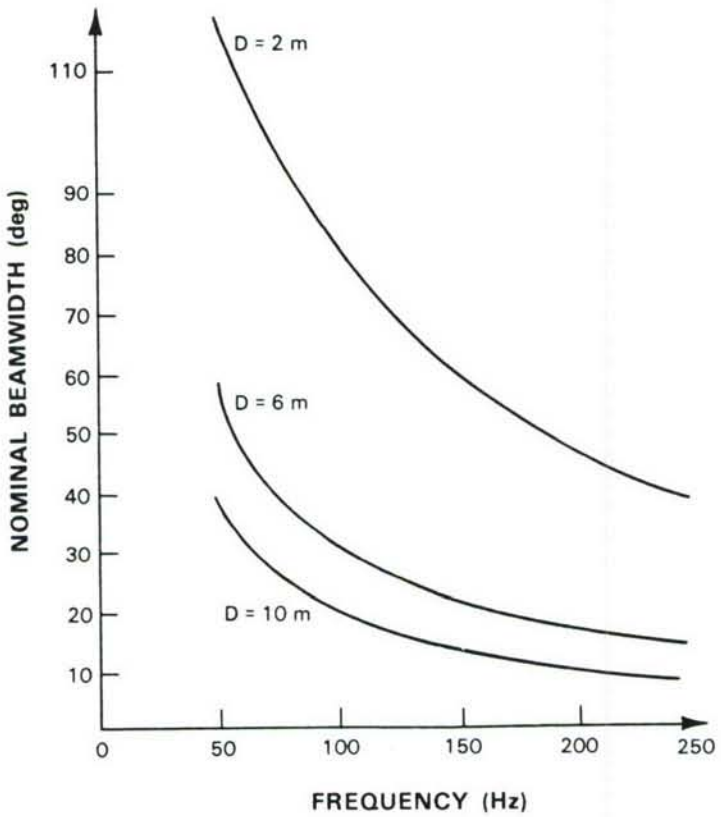

92994-9

Figure 11. Angular beamwidth for various apertures as a function of frequency.

resolved. With this in mind, compare the beamwidth of Fig. 11 for D = 6 m with the minimum azimuth resolution results of Fig. 10. The resolution obtained by the wideband algorithm is always better than the nominal resolution, even when the nominal resolution is considered only at 200 Hz. If the nominal resolution at 100 Hz is considered, the wideband algorithm is always superior by at least a factor of two. Both of these comparisons are for the low SNR case, when the wideband resolution is 15°. The resolution performance of the wideband algorithm increases substantially at higher SNRs. This behavior is not unexpected, since the MLM employed for the wave number analysis is a well-known, high-resolution method.

The results shown in Fig. 10 were obtained with no detection threshold applied to the quality measure. The primary effect of applying a detection threshold is to modify the probability that both targets will be detected and to decrease the probability of false detections when there are no targets present. Table III shows the effect on detection. The target separations shown in the table are the minimum resolvable separations for the $t = 0$ case, i.e., no threshold. Table III illustrates that for any $t < 8$ the resolution results shown on Fig. 10 do not change for SNR in the range 10 - 40 dB. For 0 dB SNR the minimum azimuth separation increases for $t > 4$.

4.5 Multiple Wideband Sources

The maximum number of equal power wideband sources that can be detected has been measured as a function of input SNR. Statistics were obtained from 50 runs per case. The maximum number of resolvable targets

TABLE III

PROBABILITY OF TWO TARGET RESOLUTION AS A FUNCTION OF A DETECTION THRESHOLD (t)

	t = 0	t = 3	t = 4	t = 6	t = 8
SNR = 40 dB azimuth separation = 6°	1.0	1.0	1.0	1.0	1.0
SNR = 20 dB azimuth separation = 9°	0.98	0.98	0.98	0.98	0.98
SNR = 10 dB azimuth separation = 12°	0.96	0.96	0.96	0.96	0.96
SNR = 0 dB azimuth separation = 15°	0.94	0.94	0.82	0.08	0.0

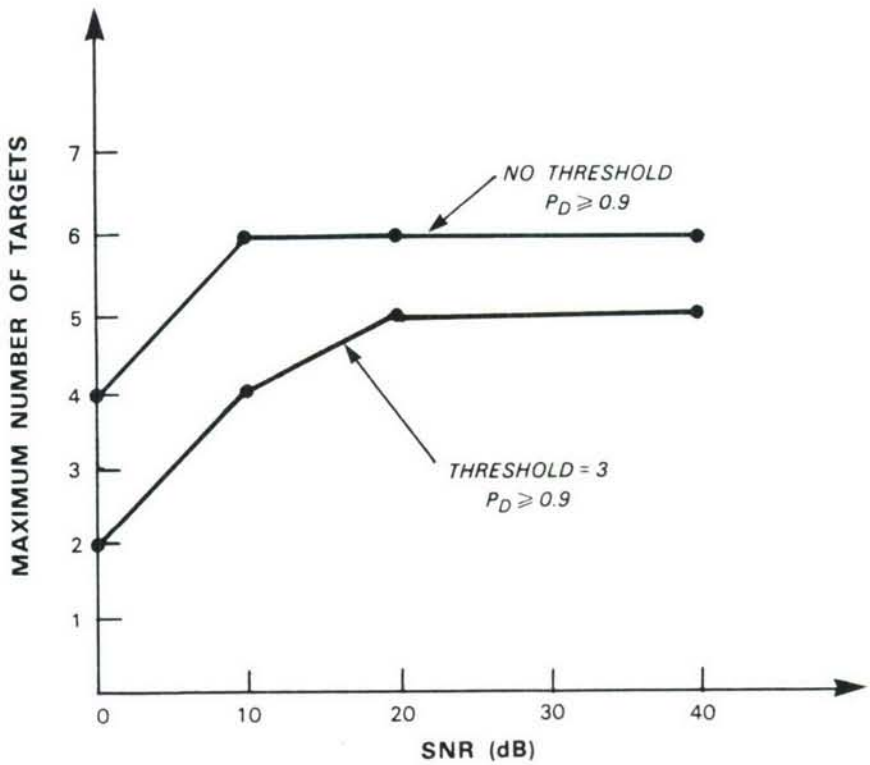

Figure 12. Maximum number of resolvable targets as a function of input SNR.

at M dB SNR was defined to be N, if at M dB SNR no more than N targets could be resolved. The azimuth estimates of the resolved targets were required with probability 0.9 (at least 45 of the 50 test cases), to have the highest quality measures.

Figure 12 shows the relationship between SNR and number of resolvable targets. One curve is with no detection threshold applied to the output quality measure, and the second is with a detection threshold of 3. When the detection threshold was applied, all targets were required to be above the threshold.

Theory suggests that the maximum number of resolvable targets is k-1 [6], where k is the number of sensors. For the array used in this report k-1 = 8. Our results indicate that only six targets can be resolved without a threshold and only five with a detection threshold of three. We believe that the reduced number of resolvable targets is due to the sidelobe structure of the array, which is not taken into account by the theory that predicts k-1 resolvable targets.

For a range of SNRs and number of targets, we examined the effect of a detection threshold applied to the output quality measure on the probability of detection (P_D) and false alarm rate (P_{FA}). For this purpose a false alarm was declared when there was any azimuth estimate above the detection threshold and unrelated to a target. In addition, the average number of false alarms - #FA - was also computed. That number was calculated as the ratio between the total number of false alarms and the number of cases in which a false alarm occurred. Results are given in Table IV.

As a graphical example of the information in Table IV, Fig. 13 shows the probability of a false alarm, and the average number of false alarms as a function of the threshold for 40 dB SNR and 5 targets. Figure 13 suggests that t = 4 might be preferred to t = 3 because of the steep drop in P_{FA} at t = 4. But recall (Table III) that t = 3 provides good detection probability for two targets with 0 dB SNR that are separated by 15 deg, but t = 4 results in reduced detection probabilities. Other two-target simulations also showed that detection probability at t = 4 did not increase, even when target separation was increased to 36°. These results indicate that t = 3 is probably a good choice for the multitarget as well as for the single target case.

Figure 14 shows the relation between maximum number of detectable targets, probability of false alarm, and the average number of false alarms, as a function of the input SNR for the case t = 3. An interesting observation can be made: the probability of false alarms decreases as the SNR decreases. The reason is that most of the false alarms at high SNR are sidelobe detections of sources, not background noise detections. Only at low input SNR, less than 10 dB, do significant numbers of the false alarms result from background noise.

TABLE IV (a)

MULTIPLE TARGET PROBABILITY OF DETECTION

	t = 0	t = 3	t = 4	t = 6	t = 8
SNR = 40	0.96	0.04	0.0	0.0	0.0
6 TARGETS					
SNR = 40	1.0	1.0	0.96	0.2	0.0
5 TARGETS					
SNR = 20	1.0	0.04	0.0	0.0	0.0
6 TARGETS					
SNR = 20	1.0	1.0	0.92	0.2	0.0
5 TARGETS					
SNR = 10	0.9	0.0	0.0	0.0	0.0
6 TARGETS					
SNR = 10	0.98	0.72	0.1	0.0	0.0
5 TARGETS					
SNR = 10	1.0	1.0	0.64	0.04	0.0
4 TARGETS					
SNR = 0	0.96	0.0	0.0	0.0	0.0
4 TARGETS					
SNR = 0	0.98	0.28	0.0	0.0	0.0
3 TARGETS					
SNR = 0	1.0	1.0	0.9	0.08	0.0
2 TARGETS					

TABLE IV (b)

MULTIPLE TARGET FALSE ALARM STATISTICS

	t = 0		t = 3		t = 4		t = 6		t = 8	
	P_{FA}	#FA	P_{FA}	#FA	P_{FA}	#FA	P_{FA}	#FA	P_{FA}	#FA
SNR = 40 6 TARGETS	1.0	5.92	0.0	-	0.0	-	0.0	-	0.0	-
SNR = 40 5 TARGETS	1.0	3.16	0.70	1.03	0.06	1.0	0.0	-	0.0	-
SNR = 20 6 TARGETS	1.0	5.81	0.0	-	0.0	-	0.0	-	0.0	-
SNR = 20 5 TARGETS	1.0	3.42	0.68	1.06	0.16	1.13	0.0	-	0.0	-
SNR = 10 6 TARGETS	1.0	5.88	0.0	-	0.0	-	0.0	-	0.0	-
SNR = 10 5 TARGETS	1.0	4.1	0.12	1.0	0.0	-	0.0	-	0.0	-
SNR = 10 4 TARGETS	1.0	3.44	0.08	1.25	0.0	-	0.0	-	0.0	-
SNR = 0 4 TARGETS	1.0	6.38	0.0	-	0.0	-	0.0	-	0.0	-
SNR = 0 3 TARGETS	1.0	6.84	0.0	-	0.0	-	0.0	-	0.0	-
SNR = 0 2 TARGETS	1.0	8.46	0.0	-	0.0	-	0.0	-	0.0	-

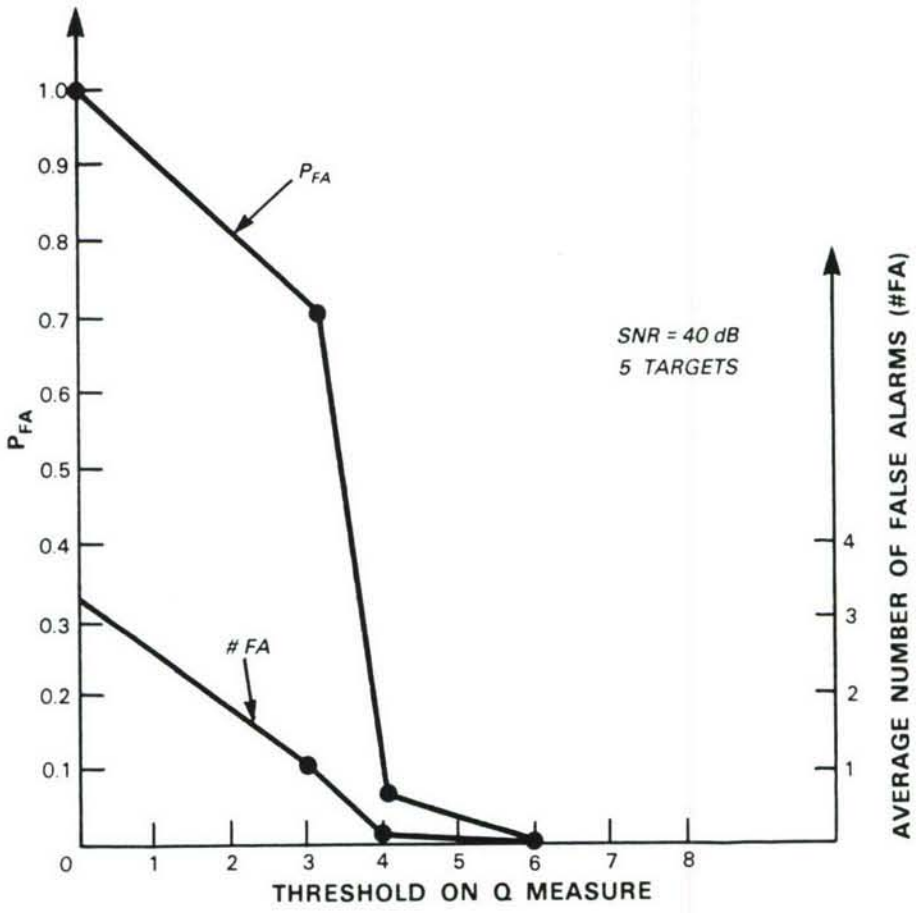

92994-10

Figure 13. Probability of false alarm and the average number of false alarms as a function of the threshold for 40 dB SNR and 5 targets.

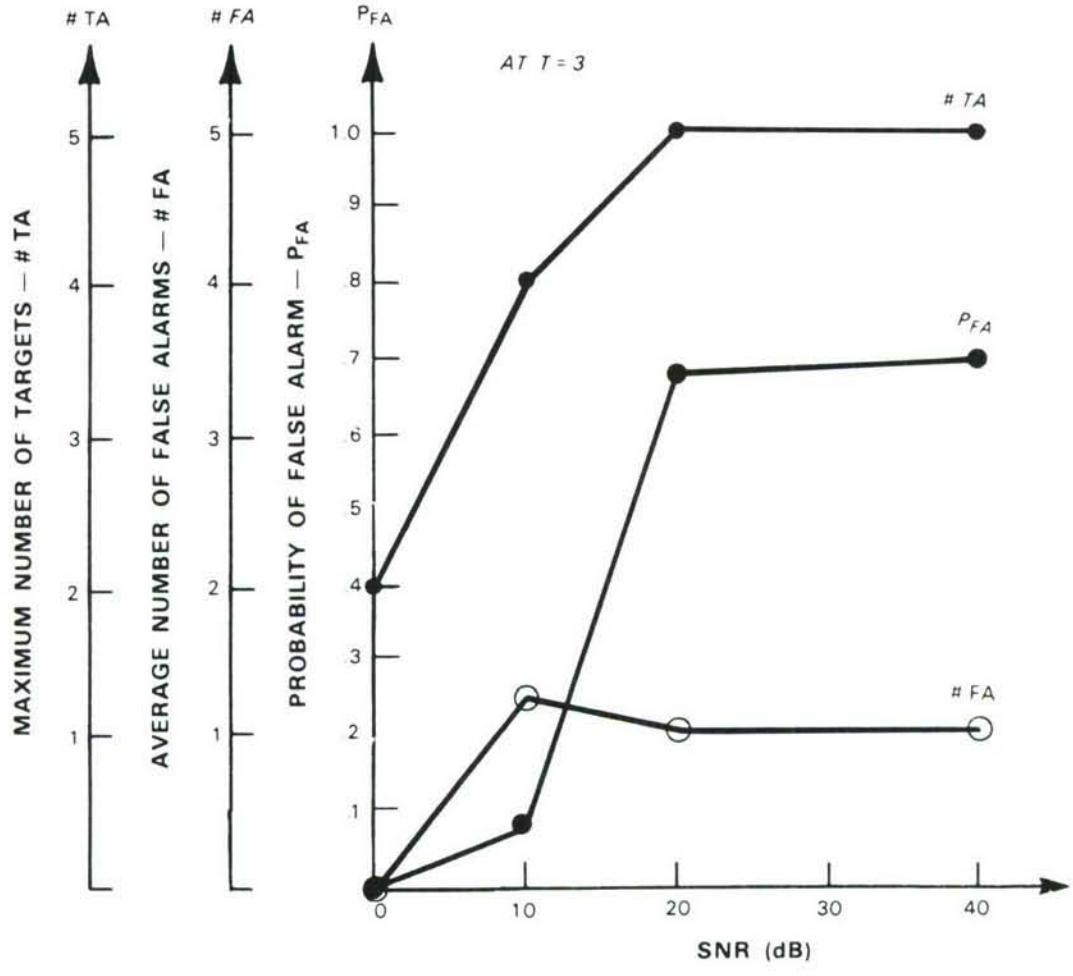

Figure 14. Maximum number of detectable targets, probability of false alarm and the average number of false alarms as a function of SNR.

5. WIDEBAND ALGORITHM COMPARED TO NARROWBAND MAXIMUM LIKELIHOOD METHOD

Two types of simulated signals have been used to compare the performance of the WB algorithm and the narrowband MLM method: a harmonic source and a wideband source. The wideband signal was white noise prefiltered to the frequency range 50 - 100 Hz. The harmonic source was a sum of equal power sine waves at 16, 32, 48, 64, 80, and 96 Hz. White noise was added at 40, 20, 0, -10 dB SNR at the input. For each SNR value 20 simulations were performed. The number of simulations was kept relatively small because of the large processing requirements of the MLM method. A block size of 128 was used in all cases of the WB algorithm and a block size of 256 was used in all cases of the MLM algorithm.

The bandwidth and structure of the harmonic source are different from those used to obtain most of the other results in this report. The WB vs narrowband MLM comparison simulations were actually performed first. Review of the initial results and actual helicopter spectra led to the selection of a different harmonic structure for subsequent simulations. In addition, separate experimental results with real data led to using a wider and higher frequency bandwidth for the subsequent simulations.

The computationally intensive WB vs MLM comparison was not repeated with the different harmonic source model or bandwidth changes because we believe that it would not change the essential conclusions. These are that the WB method is superior for wideband sources and the narrowband MLM method can be superior if the source frequencies with high SNR values are known a priori.

5.1 Harmonic Source

The wideband algorithm was applied using a 10-100 Hz bandwidth. This provided 10 dB of prefiltering SNR gain (see Table I). The MLM method was applied at each of the source frequencies (16, 32, 48... 96 Hz) and at intermediate frequencies (24, 40, 56, 72, and 88 Hz). Results are shown in Table V.

The results indicate that MLM performs better at the exact source frequencies where there is a very high SNR. For frequencies between the source harmonics, the accuracy of the wideband method compared to MLM depends on frequency. MLM is better at high frequencies, about the same at frequencies in the middle of the processing band, and worst at low frequencies. Thus, MLM can perform better by careful selection of frequencies. But if the source spectrum is known, the wideband method can also be tailored by prefiltering to improve performance.

5.2 Wideband Source

In the case of wideband sources, the wideband algorithm used the entire 50-100 Hz frequency band. The prefiltering SNR gain for this case is given in Table I as 12 dB. MLM single frequency estimates were calculated at 48, 56, 64, 72, 80, 88, 96, and 104 Hz. For each algorithm the standard deviation of the azimuth estimates from the true direction were calculated as a function of the input SNR and are given in Table VI. From these simulations we can see that the WB algorithm performs as well as or better than single frequency MLM for a white noise source.

TABLE V

STANDARD DEVIATION OF AZIMUTH ESTIMATES [deg] FOR A HARMONIC SOURCE

INPUT SNR	MLM ALGORITHM											WIDE-BAND ALGORITHM
	16 Hz	24 Hz	32 Hz	40 Hz	48 Hz	56 Hz	64 Hz	72 Hz	80 Hz	88 Hz	96 Hz	
40 dB	0.0	0.3	0.0	0.18	0.0	0.08	0.0	0.06	0.0	0.06	0.0	0.24
20 dB	0.22	3.7	0.16	1.48	0.11	0.8	0.0	0.56	0.0	0.81	0.06	1.18
0 dB	2.40	27.42	0.94	14.57	0.72	14.15	0.39	8.4	0.46	12.33	0.39	24.45
-10 dB	8.33	60.94	3.52	29.71	2.36	23.77	2.27	15.84	1.29	18.38	1.01	22.56

TABLE VI

STANDARD DEVIATION OF AZIMUTH ESTIMATES [deg] AS A FUNCTION OF SNR FOR A WIDEBAND SOURCE

INPUT SNR	MLM ALGORITHM								WIDE-BAND ALGORITHM
	48 Hz	56 Hz	64 Hz	72 Hz	80 Hz	88 Hz	96 Hz	104 Hz	
40 dB	0.	0.	0.	0.	0.	0.	0.	0.	0.
20 dB	0.207	0.0625	0.0625	0.0625	0.088	0.0625	0.	0.	0.
0 dB	1.21	0.804	0.675	0.81	0.375	0.476	0.491	0.471	0.464
-10 dB	3.97	2.6	1.61	1.91	1.21	1.79	1.96	1.37	1.199

6. SUMMARY

The performance of the WB algorithm and an ad hoc quality measure have been investigated. It appears that the quality measure will be useful to the tracker. The value was high when estimates were accurate and low when errors were large; i.e., the quality measure functioned like an output SNR measure.

In single source situations, the WB algorithm performed much better on a white wideband source than on an harmonic source. The values of the quality measure were lower for the harmonic source estimates than for the wideband source reflecting the better performance for the wideband white sources. We also found how the WB algorithm performance varied as a function of processing parameters.

Single source wideband direction determination accuracy ranged from several degrees to less than a degree, depending upon source type, SNR, and processing parameters such as block size and processing bandwidth. A detection threshold of 3 applied to the empirical quality measure substantially reduced false alarms without changing detection probability for signals with an input SNR of 0 dB or above.

In the case of two wideband sources we found that at 40 dB input SNR, targets at least 6 degrees apart could be resolved. At 0 dB SNR, target resolution was not achieved unless the separation was at least 15 deg. These numbers change as a function of the threshold applied to the output quality measure, especially at low SNR. For multiple wideband sources, we found that 6 widely spread targets can be resolved at 40 dB SNR and at 0 dB 4 targets can be resolved. Again, these numbers will change as a function of the threshold.

A comparison of the wideband method and narrowband MLM techniques showed the wideband method to be superior for wideband sources. The narrowband MLM method was superior at selected frequencies for the case of harmonic sources, although the wideband method could be made superior by prefiltering to improve SNR.

These results are a function of the number of sensors and the physical size of the array; they are not absolute characteristics for the WB algorithm.

ACKNOWLEDGMENT

I wish to thank Dr. Richard T. Lacoss for careful reading and constructive suggestions, which improved the quality of the presentation of this work, and thank Carl E. Nielsen for useful suggestions.

REFERENCES

[1] "Direction Estimation of Wideband Signals," S.H. Nawab et al., IEEE Trans. ASSP, Vol. 33 No. 5, pp. 1114-1122, 1985.

[2] "High Resolution Frequency-Wavenumber Spectrum Analysis," J. Capon, Proc. IEEE, Vol. 57 No. 8, pp. 1408-1418, 1969.

[3] Digital Signal Processing, A.V. Oppenheim and R.W. Schafer (Prentice Hall, Englewood Cliffs, N.J., 1975).

[4] Distributed Sensor Networks Semiannual Technical Summary, Lincoln Laboratory, MIT (30 September 1979), DDC AD-A086800/0.

[5] "Resolving Power and Sensitivity to Mismatch of Optimum Array Processors," H. Cox, J. Acoust Soc. Am., Vol 54, pp. 771, 1973.

[6] "Bearing Estimation of Wideband Signals by Multidimensional Spectral Analysis," F.U. Dowla, Ph.D. Thesis, MIT, Cambridge, MA, October 1984.

REPORT DOCUMENTATION PAGE

1a. REPORT SECURITY CLASSIFICATION Unclassified	1b. RESTRICTIVE MARKINGS
2a. SECURITY CLASSIFICATION AUTHORITY	3. DISTRIBUTION/AVAILABILITY OF REPORT Approved for public release; distribution unlimited.
2b. DECLASSIFICATION/DOWNGRADING SCHEDULE	
4. PERFORMING ORGANIZATION REPORT NUMBER(S) CMT-105	5. MONITORING ORGANIZATION REPORT NUMBER(S) ESD-TR-87-267
6a. NAME OF PERFORMING ORGANIZATION Lincoln Laboratory, MIT 6b. OFFICE SYMBOL *(If applicable)*	7a. NAME OF MONITORING ORGANIZATION Electronic Systems Division
6c. ADDRESS *(City, State, and Zip Code)* P.O. Box 73 Lexington, MA 02173-0073	7b. ADDRESS *(City, State, and Zip Code)* Hanscom AFB, MA 01731
8a. NAME OF FUNDING/SPONSORING ORGANIZATION Air Force Systems Command, USAF 8b. OFFICE SYMBOL *(If applicable)*	9. PROCUREMENT INSTRUMENT IDENTIFICATION NUMBER Program 331
8c. ADDRESS *(City, State, and Zip Code)* Andrews AFB Washington, DC 20334	10. SOURCE OF FUNDING NUMBERS PROGRAM ELEMENT NO. 62301E 63003F / PROJECT NO. / TASK NO. / WORK UNIT ACCESSION NO.
11. TITLE *(Include Security Classification)* Evaluation of a Wideband Direction Estimation Algorithm for Acoustic Arrays	
12. PERSONAL AUTHOR(S) Tamar Peli	
13a. TYPE OF REPORT Project Report 13b. TIME COVERED FROM _____ TO _____	14. DATE OF REPORT *(Year, Month, Day)* 11 February 1988 15. PAGE COUNT 52
16. SUPPLEMENTARY NOTATION	

17. COSATI CODES			18. SUBJECT TERMS *(Continue on reverse if necessary and identify by block number)*	
FIELD	GROUP	SUB-GROUP	acoustic target detection	MLM
			direction estimation	harmonic sources
			resolution	wideband sources

19. ABSTRACT *(Continue on reverse if necessary and identify by block number)*

In this work we evaluate the performance of an acoustic target detection and direction estimation algorithm. The accuracy of azimuth estimates for a single source and the ability to handle multiple sources was examined. Single source accuracy was measured as a function of input SNR and source types. The azimuth separation required to resolve two sources and the maximum number of widely spread (in azimuth space) sources that can be resolved were measured as a function of input SNR. The performance of the algorithm was compared to the performance of the single frequency MLM algorithm. The usefulness of an output quality measure was experimentally tested.

20. DISTRIBUTION/AVAILABILITY OF ABSTRACT ☐ UNCLASSIFIED/UNLIMITED ☒ SAME AS RPT. ☐ DTIC USERS	21. ABSTRACT SECURITY CLASSIFICATION Unclassified	
22a. NAME OF RESPONSIBLE INDIVIDUAL Lt. Col. Hugh L. Southall, USAF	22b. TELEPHONE *(Include Area Code)* (617) 981-2330	22c. OFFICE SYMBOL ESD/TML